JOURNAL OF VIROLOGY, July 2009, p. 6837–6848 Vol. 83, No. 13
0022-538X/09/$08.00+0 doi:10.1128/JVI.00379-09

Human Metapneumovirus Establishes Persistent Infection in the Lungs of Mice and Is Reactivated by Glucocorticoid Treatment▽

Yuru Liu,[1]† Debra L. Haas,[2]† Spencer Poore,[2] Sanjin Isakovic,[2] Michelle Gahan,[3] Suresh Mahalingam,[3] Zhen F. Fu,[1] and Ralph A. Tripp[2]*

Department of Pathology, College of Veterinary Medicine, University of Georgia, Athens, Georgia 30602[1]; Department of Infectious Diseases, Center for Disease Intervention, College of Veterinary Medicine, University of Georgia, Athens, Georgia 30602[2]; and Centre for Biomedical, Molecular and Chemical Sciences, University of Canberra, Canberra, ACT 2601, Australia[3]

Received 20 February 2009/Accepted 30 March 2009

Human metapneumovirus (HMPV) has been identified as a worldwide agent of serious upper and lower respiratory tract infections in infants and young children. HMPV is second only to respiratory syncytial virus (RSV) as a leading cause of bronchiolitis, and, like RSV, consists of two major genotypes that cocirculate and vary among communities year to year. Children who have experienced acute HMPV infection may develop sequelae of wheezing and asthma; however, the features contributing to this pathology remain unknown. A possible mechanism for postbronchiolitis disease is that HMPV might persist in the lung providing a stimulus that could contribute to wheezing and asthma. Using immunohistochemistry to identify HMPV-infected cells in the lungs of mice, we show that HMPV mediates biphasic replication in respiratory epithelial cells then infection migrates to neuronal processes that innervate the lungs where the virus persists with no detectable infection in epithelial cells. After glucocorticoid treatment, the virus is reactivated from neural fibers and reinfects epithelial cells. The findings show that HMPV persists in neural fibers and suggest a mechanism for disease chronicity that has important implications for HMPV disease intervention strategies.

Human metapneumovirus (HMPV), a recently recognized paramyxovirus in the *Pneumovirus* genus, was first isolated in 2001 from nasopharyngeal aspirates of young children with respiratory disease (73). HMPV is a ubiquitous and important respiratory pathogen causing upper and lower respiratory tract disease in infants and young children, but infection may also cause disease in the elderly and immunocompromised (15, 26, 38, 45, 73, 75). It is recognized that severe respiratory viral infections in childhood are associated with the development of asthma later in life (47), and HMPV disease has been implicated as a trigger for bronchiolitis and asthma in infants and young children (38, 45). These features related to HMPV infection can be severe with prolonged recovery times, a feature that is not well understood.

HMPV replication initiates in the upper respiratory tract; however, it can spread to the lower airways involving the bronchi, bronchioles, and alveoli. Evidence from experimental infection in cynomolgus macaques indicates that HMPV replication is short-lived and limited to the apical surface of ciliated respiratory epithelial cells (42). However, the various cell types that may be susceptible to HMPV infection are not completely understood. The HMPV G protein is considered to be the principal means for virus attachment to host cells, and F protein is required for penetration mediated by fusion with the plasma membrane (11, 59). Penetration requires proteolytic cleavage of the F protein, incorporation of the viral envelope into the cell membrane, nucleocapsid release into the cytoplasm, and L protein initiation of viral transcription where replication proceeds in the cytoplasm without nuclear involvement (11, 59). Virions assemble at the plasma membrane, where inclusion bodies containing viral ribonucleoprotein cores appear immediately below the plasma membrane, and nucleocapsids localize with cell membrane containing membrane viral proteins (73).

HMPV and respiratory syncytial virus (RSV) are closely related pneumoviruses that after infection cause similar clinical manifestations (46, 54, 75, 79). Given the recent discovery of HMPV (73), it is not surprising that substantially more is known about RSV infection, and it is likely that many features linked to RSV will be similar to HMPV (45). RSV and HMPV genome have been detected in chronic obstructive pulmonary disease patients (24, 25, 49, 61, 76, 78), a feature suggestive of persistent infection. In the mouse model, RSV has been shown to induce long-term airway disease characterized by chronic airway inflammation and airway hyper-reactivity, where 42 days after RSV infection reverse transcription-PCR (RT-PCR) indicated the presence of viral RNA in the lower respiratory tract, and the presence of genomic RNA persisted for months after infection (52). These findings are consistent with other findings that RSV persists in the lungs of guinea pigs 60 days after the resolution of acute bronchiolitis (17, 37), and the observation of RSV latency and persistence in the lungs of BALB/c mice despite T-cell immunity (60). Susceptibility to persistent RSV infection likely involves both host and viral factors. RSV is capable of evading immune responses by modifying cytokine and chemokine responses (67, 69, 71). Our group and others have shown that RSV antagonizes antiviral type I interferon (IFN) responses (9, 53, 64), modifies cytokine regulation through suppressor of cytokine signaling pathways

* Corresponding author. Mailing address: Animal Health Research Center, University of Georgia, 111 Carlton Street, Athens, GA 30602. Phone: (706) 542-4312. Fax: (706) 583-0176. E-mail: ratripp@uga.edu.
† Y.L. and D.H. contributed equally to this study.
▽ Published ahead of print on 8 April 2009.

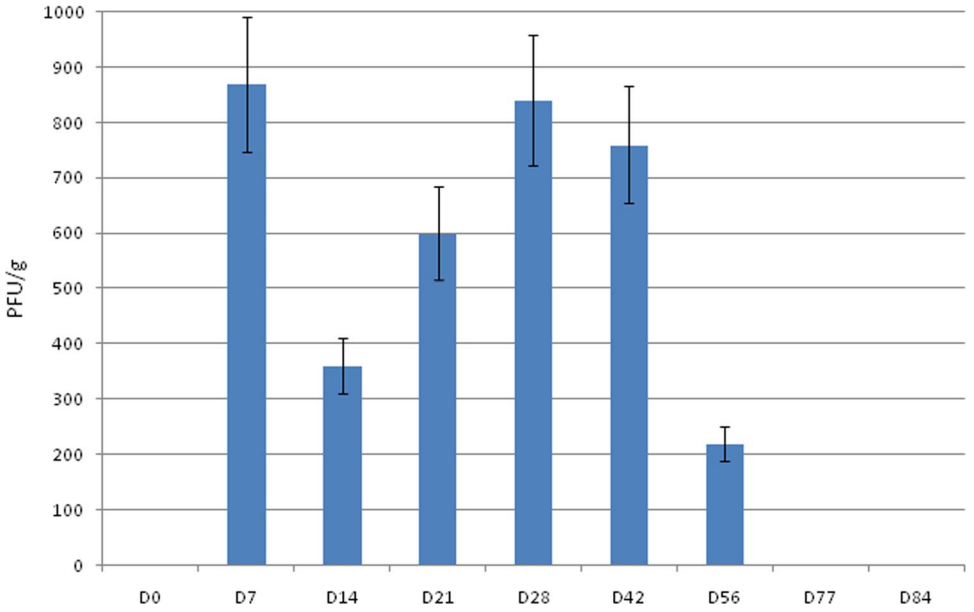

FIG. 1. Kinetics of HMPV replication in BALB/c mice as demonstrated by lung virus titers. Mice were intranasally infected with 5×10^5 PFU of HMPV/CAN97-83, and the lung titers were determined at the time points indicated by using an immunostaining plaque assay as previously described (1). The error bars indicate the standard error of the mean.

(53), mimics the activities of CX3C chemokines (68), alters pulmonary T-cell trafficking (34, 68, 70), inhibits apoptosis (28, 30), and enters immune-privileged cells such as pulmonary neurons (43, 61). RSV may also escape an established immune response through variability in envelope-associated protein genes (13, 80). Persistent HMPV infection has been documented in hematopoietic stem cell transplantation patients (20, 22), where HMPV infection in the lower respiratory tract was associated with respiratory failure in some immunocompromised adults (22), and evidence indicates that HMPV may persist the lungs of HMPV-infected mice (1, 2, 32). Like RSV, emerging studies are revealing that HMPV modulates aspects of immunity to facilitate replication, and it is possible these attributes may also contribute to persistence.

The evidence that HMPV may persist in the lungs after infection suggests that HMPV utilizes mechanisms to avoid or reduce host immunity to infection. HMPV lacks nonstructural NS1 and NS2 genes (5) that have been shown for RSV to antagonize the activities of type I IFNs (9, 29, 64). Despite the absence of this feature, HMPV appears to be able to inhibit the type I IFN antiviral response through other mechanisms. In one study that examined HMPV-infected lung epithelial cells, it was shown that HMPV is capable of regulating IFN-mediated signaling through regulation of STAT1 phosphorylation and nuclear translocation (21). In addition, HMPV G protein has recently been shown to associate with the intracellular viral RNA sensor, RIG-I, and inhibit RIG-I-dependent gene transcription and cellular signaling (4). In that study, infection of airway epithelial cells with a recombinant HMPV lacking the G protein resulted in higher levels of chemokines and type I IFNs compared to cells infected with wild-type HPMV and indicated that the G protein mediated an effect that was linked to nuclear factor (NF)-κB and IFN regulatory factor transcription factors (4).

HMPV and RSV have many similarities including clinical manifestations of disease (46, 54, 75, 79), and evidence for persistence after infection (1, 2, 17, 23, 32, 37, 60, 61). Since RSV may infect primary cortical neurons and neurons that innervate the lungs of BALB/c mice (43), we postulated that HMPV may also infect immune-privileged neuronal cells that innervate the lungs of BALB/c mice as a means to facilitate persistence. In the present study, we examine infection of BALB/c mice with strain A HMPV/CAN98-83 and show that HMPV undergoes biphasic replication of respiratory epithelia in the lung, persists in neuronal processes or fibers that innervate the lungs of mice, and can be reactivated from neuronal processes by dexamethasone (Dx) treatment leading to reinfection of respiratory epithelia and histopathology. The implications of these findings are important in understanding HMPV disease sequelae and disease chronicity and may also have important implications for patients receiving steroid treatment to reduce pulmonary inflammation or chronic obstructed airways linked to previous respiratory virus infection (33, 62).

MATERIALS AND METHODS

Animals. Four- to six-week-old, specific-pathogen-free female BALB/c mice were purchased from Harlan Sprague-Dawley Laboratories (Indianapolis, IN). The mice were housed in microisolator cages and fed sterilized water and food ad libitum. Experiments were approved by Institutional Animal Care and Use Committee at the University of Georgia.

Virus preparation and cell lines. Rhesus monkey kidney cells (LLC-MK2; ATCC CCL 7.1) were maintained in GlutaMAX-I reduced serum medium (Opti-MEM; Gibco USA) supplemented with 5% fetal bovine serum (TCM; HyClone, Logan, UT). A HMPV stock was prepared in LLC-MK2 cells by using similar methods as previously described (1). Briefly, before infection, 80% confluent LLC-MK2 cells were washed three times in serum-free Opti-MEM and then infected with strain A HMPV/CAN98-83 (HMPV) at a multiplicity of infection of 0.5. The virus was allowed to adsorb for 1.5 h at 37°C in serum-free Opti-MEM containing 2.5 μg of TPCK (tolylsulfonyl phenylalanyl chloromethyl

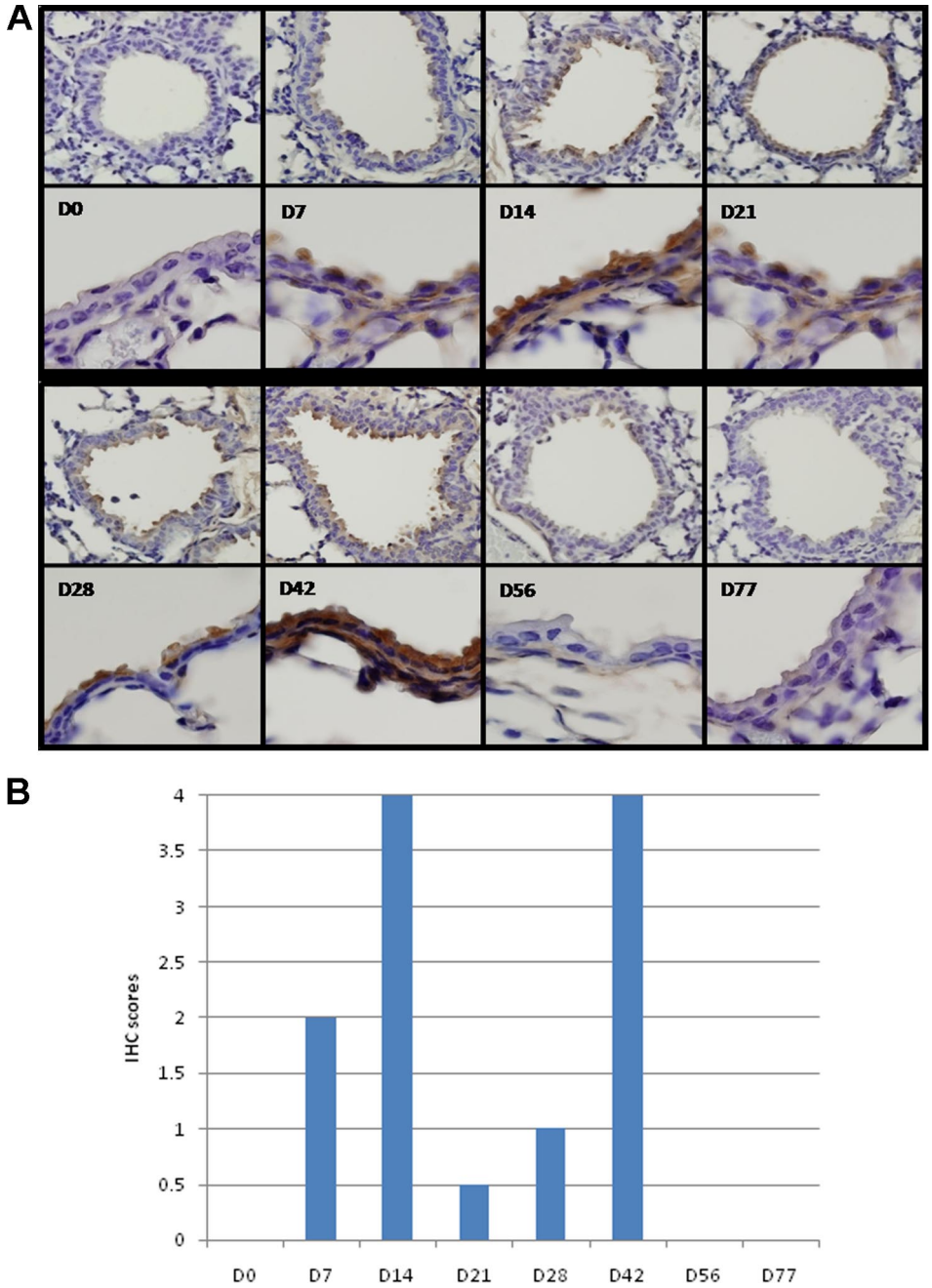

FIG. 2. IHC detection of HMPV infection in lung sections. Paraffin-embedded lung sections collected from mice at the times indicated were prepared as previously described (35, 36) and stained with rabbit antisera reactive to HMPV G protein. (A) Images (×25 magnification) of the lung section are separated by the dashed line from ×100 magnification images for each time point examined. (B) To aid interpretation, the IHC scores are indicated. IHC scores are indicated as follows: 0, no IHC staining detected or negative; 0.5, <10% cells have detectable IHC staining; 1, weak positive where 10 to 20% cells have detectable IHC staining; 2, positive where 30 to 40% cells have detectable IHC staining; 3, positive where 50 to 70% cells have detectable IHC staining; and 4, strong positive where 80 to 100% cells have detectable IHC staining.

ketone)-treated trypsin (Worthington Biochemical Corp)/ml, after which the infected cultures were incubated for 7 to 8 days in Dulbecco modified Eagle medium containing 5% heat-inactivated fetal bovine serum (TCM) and 5 μg of trypsin/ml. Infected cells were harvested by removal of the medium, replacement with a minimal volume of serum-free Opti-MEM, followed by two snap-freeze-thaw cycles at −70 and 4°C, respectively. The contents were collected, sonicated on ice by using a Handheld Sonic Dismembrator (Fisher Scientific model 100), and centrifuged at 4,000 × *g* for 20 min at 4°C to remove cell debris, and the titer was determined by plaque assay as described below.

Infection, sampling, and Dx treatment. BALB/c mice were anesthetized by intraperitoneal administration of 2,2,2-tribromoethanol (Avertin) and infected intranasally with 5×10^5 PFU of HMPV. Mice were sacrificed at days 0, 7, 10, 14, 21, 28, 56, and 77 days postinfection (p.i.) for virus titer determination, immunohistochemistry (IHC), and RT-PCR. Prior to removal of lungs, anesthetized mice were exsanguinated by severing the right caudal artery. By day 77 p.i., no detectable HMPV antigen was observed in IHC sections stained with a polyclonal antibody directed against HMPV, by a polyclonal antibody directed against HMPV G protein, or by immunostaining plaque assay of lung lysates.

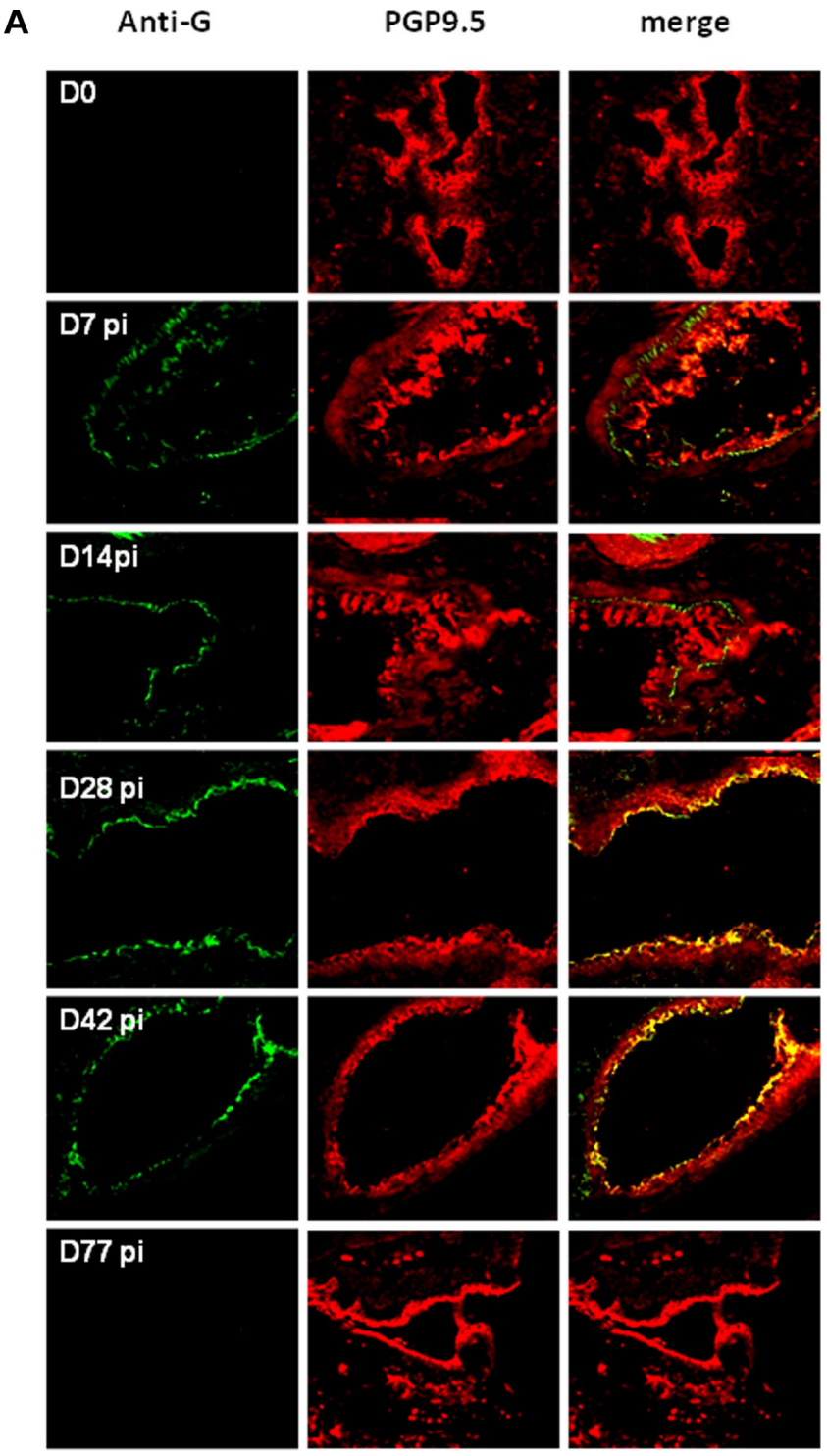

FIG. 3. IHC detection of HMPV infection in neuronal processes that innervate the lungs. (A) Lung sections were prepared from mice at the times indicated and stained with rabbit antisera reactive to HMPV G protein or using monoclonal antibody specific to the neuron marker, PGP9.5. The sections represent ×25 magnification. (B) Lung sections were evaluated for in situ hybridization of HMPV M gene genomic RNA as previously described (3). The boxes and circles indicate areas of hybridization in PGP9.5+ cells. (C) Quantitative analysis of in situ hybridization signals was determined to aid interpretation. Five images were randomly captured from each lung section; the defined image area was measured based on the fluorescence intensity, and the cumulative fluorescence was normalized to a total fluorescence distribution in 50,625-μm^2 area of tissue.

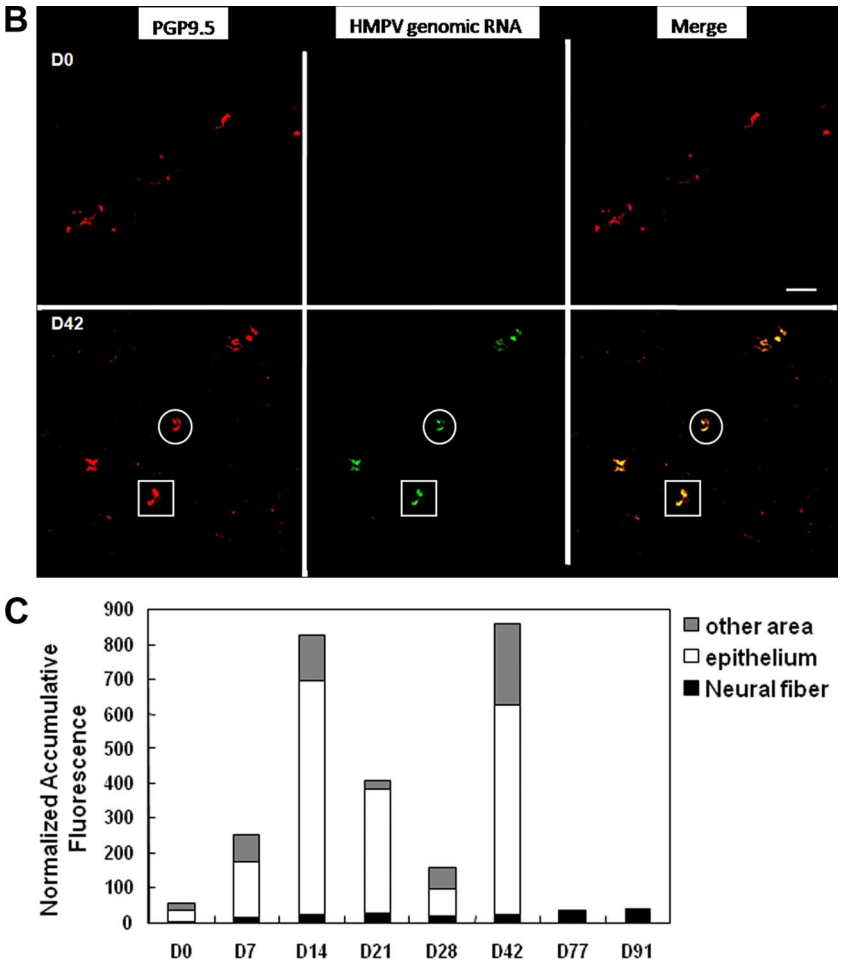

FIG. 3—*Continued.*

For Dx treatment, mice at day 77 p.i., were intravenously administered the glucocorticoid, Dx (Sigma), by tail vein injection given in three doses of 0.75 μg of Dx and 300 μl of phosphate-buffered saline (PBS) every other day for 6 days. The 3-μg dose of Dx has previously been shown to enable virus reactivation of herpes simplex virus type 1-infected mice (31, 58). Untreated mice received intravenous tail vein injections of three doses of PBS vehicle only. Both treated and untreated mice were then sacrificed at days 0 (i.e., day 77 p.i.), 4, 7, and 13 posttreatment for virus titers, IHC, and quantitative PCR analysis. Lung tissues were collected on ice in 1 ml of PBS (Gibco/Invitrogen) to determine virus titers or collected in RNA Later (Ambion, Austin, TX) for RT-PCR analysis.

Virus titers. HMPV titers from homogenized lungs were determined by immunostaining plaque assay using rabbit anti-HMPV G protein rabbit serum (Biosynthesis, Inc., Lewisville, TX) raised against two HMPV peptides, G1-17 (amino acids [aa] 1 to 17 of strain A HMPV/CAN98-83; MEVKVENIRAIDM LKAR) and G203-219 (aa 203 to 219 of strain A HMPV/CAN98-83; EETGSA NPQASVSTMQN) as previously described (8). Pooled antisera were tested by enzyme-linked immunosorbent assay (ELISA) for reactivity to the immunizing peptides, to an irrelevant peptide control, to HMPV/CAN98-83-infected LLC-MK2 cell lysate, and to uninfected LLC-MK2 cell lysate control. Briefly, HMPV-infected and uninfected lungs were collected, and 1.0 g of tissue was homogenized in 1 ml of PBS. The lung homogenates were placed on ice for 15 min to allow debris to settle. Clarified lung lysates were diluted 10-fold in serum-free Opti-MEM, added to 95% confluent LLC-MK2 cells in serum-free Opti-MEM in 24-well plates (BD Falcon, San Jose, CA), and incubated for 1 h at 37°C, followed by SeaPlaque agarose overlay in serum-free Opti-MEM containing 2.5 μg of trypsin/ml. At day 6 p.i., the overlay medium was removed from the cells on the 24-well plates, the wells were carefully washed with PBS, and the cells were fixed with acetone-methanol (60:40). After air drying, the cells were immunostained with affinity-purified rabbit anti-HMPV G protein rabbit antisera, and the plaques were enumerated with 3′,3′-diaminobenzidine (DAB; Vector Laboratories, Burlingame, CA).

IHC. For IHC staining, paraffin-embedded lung sections were prepared as described previously (35, 36). Briefly, 5-μm-lung sections were deparaffinized in xylene and hydrated in graded ethanol, followed by deionized water. Endogenous peroxidase activity was blocked by incubating the sections in 2% hydrogen peroxide in methanol for 1 min. Sections were stained overnight with appropriate dilutions of rabbit antisera reactive to HMPV G protein or using monoclonal antibodies specific to neuron marker PGP9.5 (Abcam) or an epithelial cell marker, Cytokeratin 7+ (Chemicon), as previously described (3). Biotin-conjugated goat anti-rabbit secondary antibody was applied as appropriate or used alone as a control, followed by incubation with ABC-peroxidase complex. A DAB substrate kit was used to develop coloration according to commercial recommendations (Vector Laboratories). No substantial background staining was evident with secondary antibody staining alone. Cryostat sections of 15-μm-pore-size thickness were used for colocalization studies of HMPV G protein with neuron marker PGP9.5 (Abcam) or epithelial cell marker Cytokeratin 7+ as previously described (3). Alexa Fluor 488-conjugated goat anti-rabbit or Alexa Fluor 555-conjugated goat anti-mouse secondary antibody (Invitrogen) was used to detect primary antibody staining. For in situ hybridization and IHC studies, after in situ hybridization, the sections were blocked with 5% normal goat serum and subjected to IHC staining as described above. The sections were visualized by using a Zeiss LSM 510 confocal microscope. The nuclei were counterstained with DAPI (Vector Laboratories), mounted, and analyzed.

To aid interpretation of the IHC results, all scoring was done blinded using an IHC score as follows: 0, no IHC staining detected/negative; 0.5, <10% cells have detectable IHC staining; 1, weak positive where 10 to 20% cells have detectable IHC staining; 2, positive, where 30 to 40% cells have detectable IHC staining; 3,

positive where 50 to 70% cells have detectable IHC staining; and 4, strong positive where 80 to 100% cells have detectable IHC staining.

In situ hybridization. We used 5-μm paraffin sections for in situ hybridization of HMPV M gene genomic RNA. The probes were synthesized by Invitrogen with 5′ modification of Alexa Fluor 488 or biotin. The sequences of probes were as follows: 5′-TCTGTATGCTGCATCACAAAGTGGTCCAATACTAAAAG TGAATGCATCGGCCCAG-3′ and 5′-AATCAGCCACTGTTGAAGCTGCA ATAAGCAGTGAAGCAGACCAAG-3′. In situ hybridization was performed as previously described (3). Briefly, lung sections were deparaffinized and fixed with 2% formaldehyde, followed by digestion with 10 μg of proteinase K/ml. The sections were heat treated at 98°C for 2 min to inactivate proteinase K. Subsequently, the sections were incubated with 1 pmol of probes diluted in Enoko hyb-buffer (VWR)/μl with 2% bovine serum albumin at 95°C for 5 min at 48°C for 4 h or overnight in a humidified atmosphere. The sections were washed with 2× saline sodium citrate (SSC) buffer made from a 20× stock solution consisting of 3 M sodium chloride and 300 mM trisodium citrate (adjusted to pH 7.0 with HCl) for 5 min, 1× SSC for 5 min, and 0.5× SSC for 5 min at 50°C and then examined by using a fluorescence microscope. Quantitative analysis of in situ hybridization signals were calculated by using LSM 510 software Histo-program (Zeiss). Five images were randomly captured from each section. The defined area of images was measured based on the fluorescence intensity, and the cumulative fluorescence was normalized to a total fluorescence distribution in a 50,625-μm^2 area of tissue.

RT-PCR analysis. Total RNA was isolated from HMPV-infected BALB/c lung tissue utilizing a commercial RNA isolation kit (Totally RNA; Ambion, Austin, TX) according to the manufacturer's protocol. Briefly, RT-PCR primers were generated to the N gene of strain A HMPV/CAN98-83. HMPV N gene forward primer (5′-CACCGGCAAAGCATTAGGCTCATC-3′) and reverse primer (5′-TTTGGGCTTTGCCTTAAATG-3′) were used for RT, followed by 35 cycles of PCR. For RNA quality control, the housekeeping gene GAPDH (glyceraldehyde-3-phosphate dehydrogenase) was amplified by using the GAPDH forward primer (5′-GGGTGGAGCCAAACGGTC-3′) and the GAPDH reverse primer (5′-GGAGTTGCTGTTGAAGTCGCA-3′). Plasmid DNA containing the HMPV N gene was used to generate a standard curve, based on genome copy number using the HMPV N gene forward primer (5′-GCAGCAAAGCAGAA AGTTTATTCGT-3′), reverse primer (5′-CCCACCTCAGCATTGTTTGAC-3′), and probe labeled with the dye FAM (5′-CAGCACCGTAAGCTT-3′; Applied Biosystems, Foster City, CA).

Statistical analysis. Lungs were collected from six animals/time point/experiment in three to four separate experiments. All experiments were performed in triplicate, and the mean values ± the standard deviation determined for three separate assays. Statistical significance was determined by using a Student *t* test, where a *P* value of <0.05 was considered statistically significant.

RESULTS

Lung virus titers after HMPV infection. Previous findings from our laboratory examining HMPV/CAN98-75 replication in BALB/c mice showed that HMPV replicated in lung tissues with biphasic kinetics where infectious virus was recovered out to day 60 p.i. despite the presence of HMPV-specific and neutralizing antibodies (1). In the present study, lung virus titers in BALB/c mice intranasally infected with 5×10^5 PFU HMPV/CAN97-83 were determined at days 0 to 84 p.i. by immunostaining plaque assay (1, 2). Similar to our previous findings (1), HMPV/CAN97-83 (HMPV) replicated in a biphasic mode with peak virus titers occurring at days 7 and 28 p.i. (Fig. 1). The first peak of virus replication was evident in the lungs at day 7 p.i. However, by day 14 p.i., lung virus titers decreased but then increased at day 21 p.i. where a second peak in virus titer occurred at day 28 pi. Lung virus titers remained high out to day 42 p.i. but had considerably decreased at day 56 p.i. and were undetectable at day 77 and 84 p.i. (Fig. 1). These results suggest that HMPV persists to day 56 p.i., a feature similar to that shown for HMPV/CAN98-75 infection in mice (2).

IHC detection of HMPV infection. To determine the degree of HMPV infection in the lungs, lung sections from mice infected with HMPV at days 0 to 77 p.i. were evaluated by IHC and scored as indicated in Materials and Methods. Similar to the lung virus titers that showed biphasic replication (Fig. 1), biphasic HMPV infection of respiratory epithelial cells was detected by IHC with peak antigen staining occurring at days 14 and 42 p.i. (Fig. 2). HMPV infection was detected by IHC at day 7 p.i., where 30 to 40% of the cells had detectable IHC staining (Fig. 2B). By day 14 p.i., 80 to 100% of the cells were strongly positive for IHC staining; however, by day 21 p.i., $<10\%$ of the cells had detectable IHC staining. The cells in lung sections were weakly positive at day 28 p.i., where 10 to 20% cells had detectable IHC staining; however, at day 42 p.i., 80 to 100% of the cells were strongly positive for IHC staining (Fig. 2). Weak to no IHC staining was detected at day 56 p.i., no IHC staining was evident at day 77 p.i. (Fig. 2), and no IHC staining was detected at time points out to day 98 p.i. (data not shown). In general, the lung virus titers (Fig. 1) followed a similar trend as the IHC staining of respiratory epithelial cells (Fig. 2) where there were early and late peaks of detection. A possible explanation for the differences in kinetics of IHC and virus detection may be that HMPV enters a persistent state in the lungs of infected mice. Persistent infections may involve stages of both silent and productive infection without producing damage to the host cells and can be maintained by modulation of virus and host gene expression and modification of the host immune response.

Detection of HMPV infection of PGP9.5$^+$ neuronal cells. The evidence for biphasic replication of HMPV in the lungs of infected mice (Fig. 1 and 2), and the previous findings of persistent infection despite the presence of an anti-HMPV immune response (1, 2) indicate that HMPV can evade immunity. One potential mechanism of immune evasion is infection of immune-privileged cells such as neuronal processes that innervate the lungs. Since HMPV and RSV are closely related pneumoviruses that cause similar clinical manifestations (46, 54, 75, 79), and RSV has been shown to infect PGP9.5$^+$ neuronal processes that innervate the lungs of mice, lung sections were examined for evidence of HMPV infection of neuronal cells at days 0 to 77 p.i. In these studies, lung sections were stained for the expression of PGP 9.5, a neuron-specific marker (19, 77), or HMPV G protein (Fig. 3A). The results showed HMPV G protein staining in the respiratory epithelia at days 7 to 42 p.i., a feature correlating with detection of virus over this period (Fig. 1 and 2) and, as expected, PGP9.5$^+$ staining of lung sections was evident at all time points examined (Fig. 3A). Of note, HMPV G protein detection merged with PGP9.5$^+$ staining at days 28 to 42 p.i., indicating HMPV infection of neuronal cell processes innervate the lungs.

In situ hybridization was performed to confirm the presence of HMPV genomic RNA in PGP9.5$^+$ cells in the lung sections at days 0 to 91 p.i. Hybridization signals from the HMPV M gene were measured based on the fluorescence intensity and the cumulative fluorescence normalized to a total fluorescence distribution in 50,625-μm^2 area of tissue. The results are shown for day 42 p.i. (Fig. 3B) and confirm that PGP9.5$^+$ neuronal cells harbor HMPV genomic RNA. Evaluating the distribution of HMPV genomic RNA across the tissue slice revealed that the majority of signal occurred along the epithelium with a very small fraction of signal in neural fibers; however, no HMPV genomic RNA was detectable in epithelial cells at days 77 or

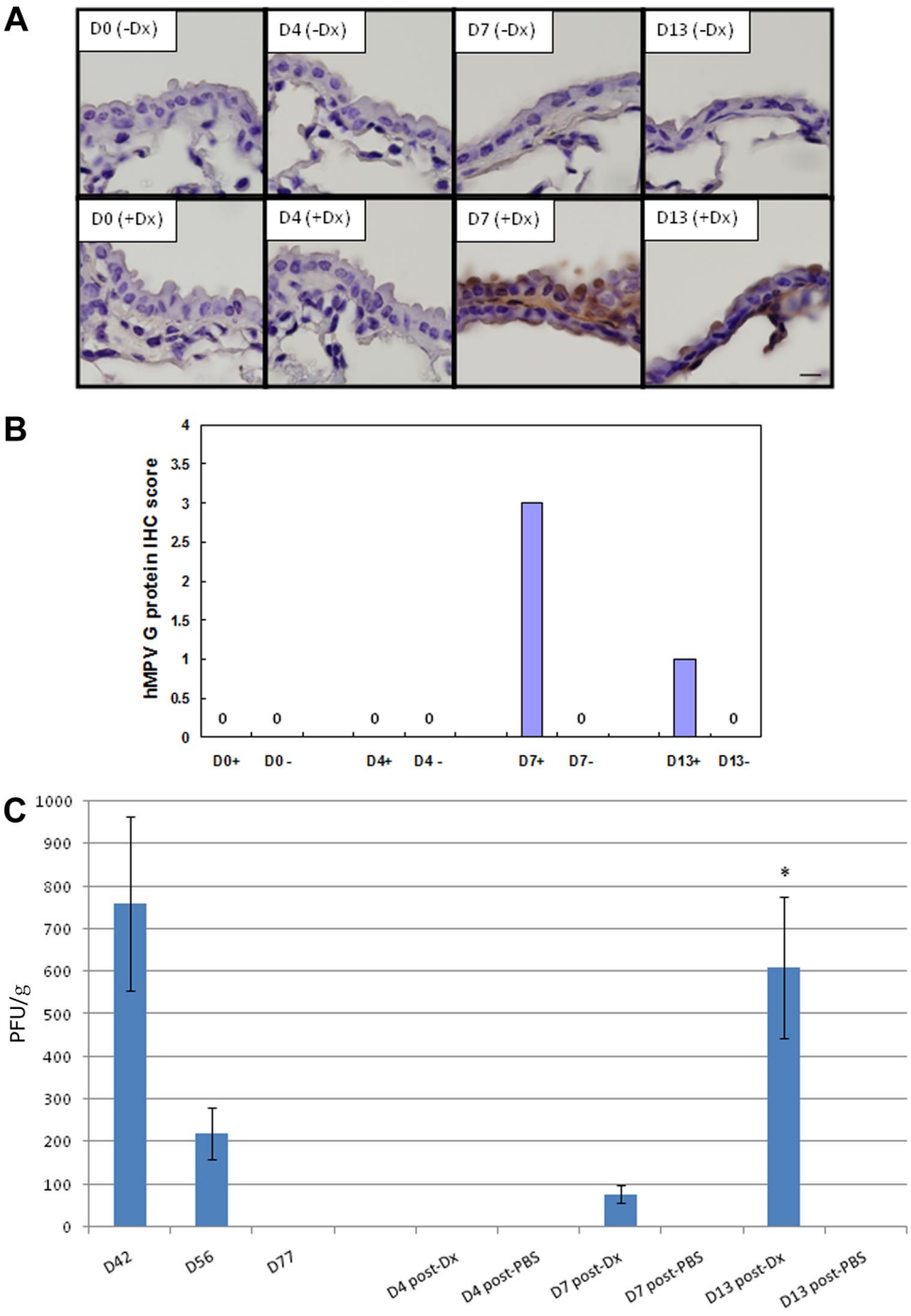

FIG. 4. IHC detection of HMPV infection and lung virus titers following glucocorticoid reactivation of HMPV. Lung sections were collected from mice at the times indicated after Dx (+Dx) or PBS (−Dx) treatment and stained with rabbit antisera reactive to HMPV G protein. (A) Images (×100 magnification) of the lung sections are shown. (B) To aid interpretation, the IHC scores are indicated as follows: 0, no IHC staining detected or negative; 0.5, <10% cells have detectable IHC staining; 1, weak positive where 10 to 20% cells have detectable IHC staining; 2, positive where 30 to 40% cells have detectable IHC staining; 3, positive where 50 to 70% cells have detectable IHC staining; and 4, strong positive where 80 to 100% cells have detectable IHC staining. +, Dx treatment; −, no Dx treatment. (C) Lung virus titers steroid activation. Lung virus titers were determined at days 4, 7, or 13 posttreatment by using immunostaining plaque assay as previously described (1). The error bars indicate the standard error of the mean. The asterisk indicates significant ($P < 0.05$) differences between day 13 and day 4 lung virus titers after Dx treatment.

91 p.i. (Fig. 3C). Interestingly, peak M gene signal correlated with IHC staining over the course of infection but was delayed relative to peak lung virus titers, an effect that may be linked to the persistent state of HMPV infection.

HMPV is reactivated after steroid treatment. To determine whether HMPV could be reactivated from the lungs of infected mice at a time point where no infectious virus (Fig. 1) or infection could be detected by IHC (Fig. 2), and no

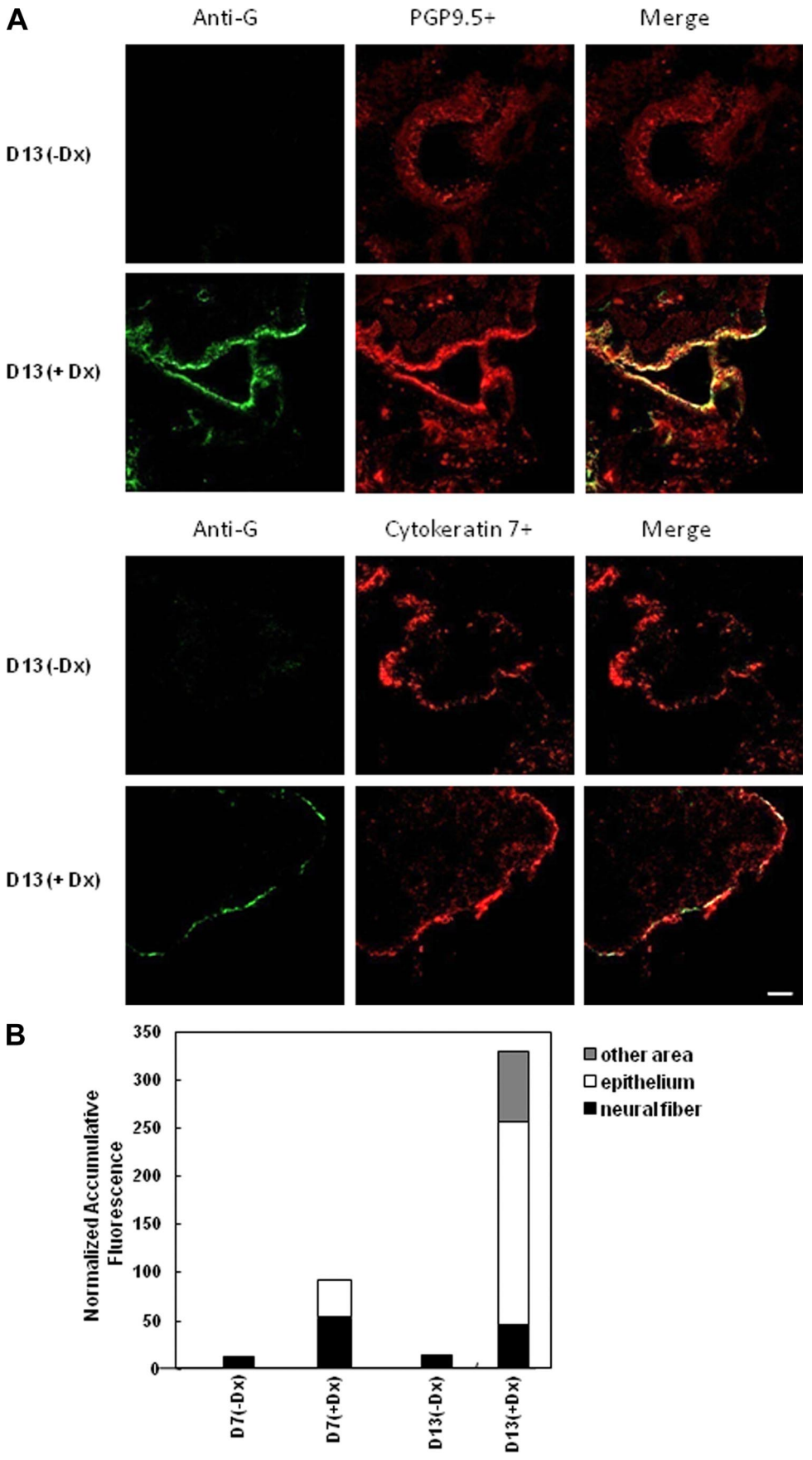
A
Anti-G
PGP9.5+
Merge
D13(-Dx)
D13(+Dx)
Anti-G
Cytokeratin 7+
Merge
D13(-Dx)
D13(+Dx)
B
Normalized Accumulative Fluorescence
350
300
250
200
150
100
50
0
other area
epithelium
neural fiber
D7(-Dx)
D7(+Dx)
D13(-Dx)
D13(+Dx)

genomic RNA was detectable in epithelial cells (Fig. 3C), HMPV-infected mice at day 77 p.i. were intravenously treated with the glucocorticoid Dx using a dose and regimen that has previously been shown to enable reactivation of herpes simplex virus type 1 from infected mice (31, 58). Control untreated mice received intravenous tail vein injections of PBS vehicle only. Both treated and untreated mice were then sacrificed at day 0 (day 77 p.i.), day 4 (day 81 p.i.), day 7 (day 84 p.i.), or day 13 (day 90 p.i.) posttreatment to determine reactivation assessed by IHC and lung virus titers (Fig. 4A). The results show that treatment with Dx, but not PBS, reactivates HMPV as detected by IHC staining of respiratory epithelial cells at day 7 and day 13 post-Dx treatment (Fig. 4A). Based on IHC score, at day 7 post-Dx treatment, 50 to 70% of the respiratory epithelial cells had detectable IHC staining, and at day 13 posttreatment, 10 to 20% of the cells had detectable IHC staining (Fig. 4B). Similar to IHC findings, no infectious virus in the lungs was detected at day 4 post-Dx treatment; however, infectious virus was detected at day 7 post-Dx treatment, and significantly ($P < 0.05$) higher levels of virus were detected at day 13 post-Dx treatment (Fig. 4C). These results show that persistent HMPV infection in the lung can be reactivated by treatment with a steroid, a feature likely related to the immunosuppressive nature of the steroid (14, 31, 58).

In situ hybridization was performed with the HMPV M gene probe to confirm the presence of HMPV genomic RNA in PGP9.5$^+$ neuronal processes or Cytokeratin 7+ respiratory epithelial cells after Dx treatment (Fig. 5). The results are shown for day 13 post-Dx or PBS treatment (or day 90 p.i.) since this time point had the highest HMPV virus titers after reactivation with Dx (Fig. 4C). As expected, no HMPV genomic RNA was detectable in PBS vehicle-treated mice; however, HMPV genomic RNA was readily detected in PGP9.5+ neuronal processes and in Cytokeratin 7+ respiratory epithelial cells in Dx-treated mice (Fig. 5A). Evaluating the distribution of HMPV genomic RNA across the tissue slice revealed signal occurring in epithelial and neural fibers at day 7 post-Dx treatment; however, substantially higher signal was evident in the respiratory epithelium at day 13 post-Dx treatment (Fig. 5B). These results indicate that HMPV persists in neuronal process and, after Dx treatment, HMPV moves from neuronal processes to infect the surrounding respiratory epithelia.

DISCUSSION

HMPV is represented by two genotypes with prototypical members, including HMPV/CAN97-83 and HMPV/CAN98-75 (7, 63). The overall level of genome nucleotide sequence identity and amino acid sequence identity between HMPV/CAN97-83 and HMPV/CAN98-75 subgroups has been shown to be 80 and 90%, respectively, with the greatest diversity between these subgroups reported for the G and SH proteins, i.e., 59 and 37% identity, respectively (7). HMPV/CAN97-83 and HMPV/CAN98-75 exhibit ca. 48% antigenic relatedness based on reciprocal cross-neutralization assays with postinfection hamster sera, and 64 to 99% antigenic relatedness based on cross-neutralization assays with postinfection sera from all three primate species (63). The expected biphasic replication for HMPV/CAN97-83 and HMPV/CAN98-75 as previously reported by our group has not been reported in other studies in mice. In one study examining the contribution of T cells to antiviral immunity and pathogenesis after HMPV/CAN97-83 infection of 6- to 7-week-old BALB/c mice, the HMPV titers were shown to peak at day 4 p.i. and remain unresolved, whereas low levels of HMPV were detected out to day 21 p.i. as determined by a 50% tissue culture infective dose assay using LLC-MK2 cells (39). It is possible that the HMPV strain, the time course being evaluated, the methods of virus detection, and/or age of the mice used in the studies may contribute to the differences in HMPV replication observed among studies. For example, in one study that examined age-associated aggravation of clinical disease after HMPV infection, infection of 8-week-old BALB/c mice with a novel subgroup A2 strain of HMPV(C4-CJP05) was delayed compared to 18-month-old mice, although lung virus titers were only evaluated out to day 9 p.i. (18). It is also possible that the dose of virus administered at infection contributes to the differences in the kinetics of peak lung virus expression. For example, in the study reported here mice were intranasally inoculated with 5×10^5 PFU HMPV/CAN97-83, and peak virus titers were observed at days 7 and 28 p.i., while in a related study previously reported from our laboratory (1), mice were intranasally inoculated with 10^6 PFU HMPV/CAN98-75, and peak virus titers were observed at days 7 and 14 p.i.

The finding in the present study that HMPV infects and persists in neuronal cell processes that innervate the lungs is important for understanding some of the potential mechanisms that may contribute to clinical disease. HMPV shares epidemiological and clinical traits with RSV causing clinical symptoms ranging from upper respiratory tract disease to severe bronchiolitis and pneumonia and may exacerbate chronic obstructive pulmonary disease (6, 12, 48, 51, 57, 61, 73). RSV has been shown to persist in a variety of cells and animal models (10, 17, 37, 60, 61, 66, 72), and infection with RSV has been shown to induce acute and chronic airway disease correlated with pulmonary function abnormalities (23, 52). Since HMPV can cause persistent infection (1, 2, 32), this suggests that persistence may be a potential mechanism that could contribute to post-bronchiolitis disease. Persistent infections

FIG. 5. IHC detection of HMPV infection in respiratory epithelial cells and neuronal processes following glucocorticoid reactivation. (A) Lung sections were prepared from mice at day 13 posttreatment with Dx (+Dx) or PBS (–Dx) and stained with rabbit antisera reactive to HMPV G protein, using monoclonal antibody specific to the neuron marker, PGP9.5, or an antibody specific for Cytokeratin 7+. The sections represent ×25 magnification. (B) Lung sections were evaluated for in situ hybridization of HMPV M gene genomic RNA, and quantitative analysis of in situ hybridization signals was performed to aid interpretation. Five images were randomly captured from each lung section, the defined image area was measured based on the fluorescence intensity, and the cumulative fluorescence was normalized to a total fluorescence distribution in 50,625 μm^2 area of tissue.

by paramyxoviruses are well documented and are often attributed to IFN antagonism by nonstructural (NS) proteins (27, 40, 41, 44, 55, 56) and, for RSV, the attachment G protein and NS proteins have been shown to modify the type I IFN response associated with suppressor of cytokine signaling proteins and IFN-stimulated gene 15 (53). Recently, HMPV has been shown to subvert type I IFN signaling by a mechanism distinct from other paramyxoviruses (21). In that study, HMPV infection was shown to prevent IFN-α-induced phosphorylation and nuclear translocation of STAT1. These findings may provide important insights into the mechanisms associated with HMPV persistence. One consequence of persistent HMPV infection is that persistence may allow for accumulation of viral mutants with better fitness, which may lead to other phenotypes such as nonsyncytial plaque mutants (50), alternatively the accumulation of mutants may allow for persistence. The findings that neuronal cells express several β1 integrins, including α5/β1 (65), is consistent with integrins α5/β1 promoting infection by HMPV (16).

In situ hybridization analysis detected HMPV genome in the lungs of infected mice out to day 91 p.i. and indicated that respiratory epithelial cells lining the airways contained the majority of HMPV genome out to day 77 p.i., after which HMPV genome could only be detected in neuronal processes. Notably, no evidence of HMPV infection was detected at day 77 p.i. or beyond as determined by IHC staining or by immunostaining plaque assay. However, Dx treatment of HMPV-infected mice at day 77 p.i. enabled reactivation of HMPV that led to substantial lung virus titers at days 7 and 13 posttreatment and reinfection of the surrounding respiratory epithelia at day 13 p.i. as determined by in situ hybridization analysis. These findings support the observation of immune control of persistent HMPV infection as we previously reported (2) and have important implications in disease intervention strategies.

Vaccine studies with cynomolgus macaques which had been vaccinated three times with HMPV within a 10-week period showed no protection against HMPV challenge 8 months after the last boost (74). This result was interpreted as transient immunity despite data showing virus neutralizing antibody titers measured at 8 months that were in the same range as those measured 4 to 6 weeks after the primary infections where the animals were protected (74). In addition, in that study HMPV genome was detectable in macaques challenged 6 weeks or 8 months after the previous infections, while virus neutralizing antibody titers were still present. These results were interpreted as an indication that a certain threshold of virus neutralizing antibody titers is required for protection; however, these results may reflect persistent HMPV infection in the animals and potentially infection of cell types that are immune privileged, as shown in the present study and indicated or implied in other studies (1, 2, 32).

In summary, a better understanding of the mechanisms that contribute to HMPV persistence and its ability to infect neuronal processes that innervate the lungs will likely be beneficial to advance our understanding of the pathophysiology associated with HMPV infection, as well as in the development of disease intervention strategies.

ACKNOWLEDGMENT

We thank the Georgia Research Alliance, which supported aspects of this study.

REFERENCES

1. **Alvarez, R., K. S. Harrod, W. J. Shieh, S. Zaki, and R. A. Tripp.** 2004. Human metapneumovirus persists in BALB/c mice despite the presence of neutralizing antibodies. J. Virol. **78:**14003–14011.
2. **Alvarez, R., and R. A. Tripp.** 2005. The immune response to human metapneumovirus is associated with aberrant immunity and impaired virus clearance in BALB/c mice. J. Virol. **79:**5971–5978.
3. **Bagasra, O.** 2007. Protocols for the in situ PCR-amplification and detection of mRNA and DNA sequences. Nat. Protocols **2:**2782–2795.
4. **Bao, X., T. Liu, Y. Shan, K. Li, R. P. Garofalo, and A. Casola.** 2008. Human metapneumovirus glycoprotein G inhibits innate immune responses. PLoS Pathog. **4:**e1000077.
5. **Bastien, N., S. Normand, T. Taylor, D. Ward, T. C. Peret, G. Boivin, L. J. Anderson, and Y. Li.** 2003. Sequence analysis of the N, P, M, and F genes of Canadian human metapneumovirus strains. Virus Res. **93:**51–62.
6. **Beckham, J. D., A. Cadena, J. Lin, P. A. Piedra, W. P. Glezen, S. B. Greenberg, and R. L. Atmar.** 2005. Respiratory viral infections in patients with chronic, obstructive pulmonary disease. J. Infect. **50:**322–330.
7. **Biacchesi, S., M. H. Skiadopoulos, G. Boivin, C. T. Hanson, B. R. Murphy, P. L. Collins, and U. J. Buchholz.** 2003. Genetic diversity between human metapneumovirus subgroups. Virology **315:**1–9.
8. **Biacchesi, S., M. H. Skiadopoulos, L. Yang, E. W. Lamirande, K. C. Tran, B. R. Murphy, P. L. Collins, and U. J. Buchholz.** 2004. Recombinant human Metapneumovirus lacking the small hydrophobic SH and/or attachment G glycoprotein: deletion of G yields a promising vaccine candidate. J. Virol. **78:**12877–12887.
9. **Bossert, B., S. Marozin, and K. K. Conzelmann.** 2003. Nonstructural proteins NS1 and NS2 of bovine respiratory syncytial virus block activation of interferon regulatory factor 3. J. Virol. **77:**8661–8668.
10. **Bramley, A. M., T. Z. Vitalis, B. R. Wiggs, and R. G. Hegele.** 1999. Effects of respiratory syncytial virus persistence on airway responsiveness and inflammation in guinea pigs. Eur. Respir. J. **14:**1061–1067.
11. **Buchholz, U. J., K. Nagashima, B. R. Murphy, and P. L. Collins.** 2006. Live vaccines for human metapneumovirus designed by reverse genetics. Expert Rev. Vaccines **5:**695–706.
12. **Camargo, C. A., Jr., A. A. Ginde, S. Clark, C. P. Cartwright, A. R. Falsey, and D. E. Niewoehner.** 2008. Viral pathogens in acute exacerbations of chronic obstructive pulmonary disease. Intern. Emerg. Med. **3:**355–359.
13. **Cane, P. A., and C. R. Pringle.** 1995. Evolution of subgroup A respiratory syncytial virus: evidence for progressive accumulation of amino acid changes in the attachment protein. J. Virol. **69:**2918–2925.
14. **Cole, T. J.** 2006. Glucocorticoid action and the development of selective glucocorticoid receptor ligands. Biotechnol. Annu. Rev. **12:**269–300.
15. **Crowe, J. E., Jr.** 2004. Human metapneumovirus as a major cause of human respiratory tract disease. Pediatr. Infect. Dis. J. **23:**S215–S221.
16. **Cseke, G., M. S. Maginnis, R. G. Cox, S. J. Tollefson, A. B. Podsiad, D. W. Wright, T. S. Dermody, and J. V. Williams.** 2009. Integrin alphavbeta1 promotes infection by human metapneumovirus. Proc. Natl. Acad. Sci. USA **106:**1566–1571.
17. **Dakhama, A., T. Z. Vitalis, and R. G. Hegele.** 1997. Persistence of respiratory syncytial virus (RSV) infection and development of RSV-specific IgG1 response in a guinea-pig model of acute bronchiolitis. Eur. Respir. J. **10:**20–26.
18. **Darniot, M., C. Pitoiset, T. Petrella, S. Aho, P. Pothier, and C. Manoha.** 2009. Age-associated aggravation of clinical disease after primary metapneumovirus infection of BALB/c mice. J. Virol. **83:**3323–3332.
19. **Day, I. N.** 1992. Enolases and PGP9.5 as tissue-specific markers. Biochem. Soc. Trans. **20:**637–642.
20. **Debiaggi, M., F. Canducci, M. Sampaolo, M. C. Marinozzi, M. Parea, C. Terulla, A. A. Colombo, E. P. Alessandrino, L. Z. Bragotti, M. Arghittu, A. Goglio, R. Migliavacca, E. Romero, and M. Clementi.** 2006. Persistent symptomless human metapneumovirus infection in hematopoietic stem cell transplant recipients. J. Infect. Dis. **194:**474–478.
21. **Dinwiddie, D. L., and K. S. Harrod.** 2008. Human metapneumovirus inhibits IFN-alpha signaling through inhibition of STAT1 phosphorylation. Am. J. Respir. Cell Mol. Biol. **38:**661–670.
22. **Englund, J. A., M. Boeckh, J. Kuypers, W. G. Nichols, R. C. Hackman, R. A. Morrow, D. N. Fredricks, and L. Corey.** 2006. Brief communication: fatal human metapneumovirus infection in stem-cell transplant recipients. Ann. Intern. Med. **144:**344–349.
23. **Estripeaut, D., J. P. Torres, C. S. Somers, C. Tagliabue, S. Khokhar, V. G. Bhoj, S. M. Grube, A. Wozniakowski, A. M. Gomez, O. Ramilo, H. S. Jafri, and A. Mejias.** 2008. Respiratory syncytial virus persistence in the lungs correlates with airway hyperreactivity in the mouse model. J. Infect. Dis. **198:**1435–1443.
24. **Falsey, A. R.** 2008. Human metapneumovirus infection in adults. Pediatr. Infect. Dis. J. **27:**S80–S83.
25. **Falsey, A. R., M. A. Formica, P. A. Hennessey, M. M. Criddle, W. M.**

Sullender, and E. E. Walsh. 2006. Detection of respiratory syncytial virus in adults with chronic obstructive pulmonary disease. Am. J. Respir. Crit. Care Med. **173:**639–643.
26. **Falsey, A. R., and E. E. Walsh.** 2006. Viral pneumonia in older adults. Clin. Infect. Dis. **42:**518–524.
27. **Fontana, J. M., B. Bankamp, and P. A. Rota.** 2008. Inhibition of interferon induction and signaling by paramyxoviruses. Immunol. Rev. **225:**46–67.
28. **Fuentes, S., K. C. Tran, P. Luthra, M. N. Teng, and B. He.** 2007. Function of the respiratory syncytial virus small hydrophobic protein. J. Virol. **81:** 8361–8366.
29. **Gotoh, B., T. Komatsu, K. Takeuchi, and J. Yokoo.** 2001. Paramyxovirus accessory proteins as interferon antagonists. Microbiol. Immunol. **45:**787–800.
30. **Groskreutz, D. J., M. M. Monick, T. O. Yarovinsky, L. S. Powers, D. E. Quelle, S. M. Varga, D. C. Look, and G. W. Hunninghake.** 2007. Respiratory syncytial virus decreases p53 protein to prolong survival of airway epithelial cells. J. Immunol. **179:**2741–2747.
31. **Halford, W. P., B. W. Gebhardt, and D. J. Carr.** 1996. Mechanisms of herpes simplex virus type 1 reactivation. J. Virol. **70:**5051–5060.
32. **Hamelin, M. E., G. A. Prince, A. M. Gomez, R. Kinkead, and G. Boivin.** 2006. Human metapneumovirus infection induces long-term pulmonary inflammation associated with airway obstruction and hyperresponsiveness in mice. J. Infect. Dis. **193:**1634–1642.
33. **Hanania, N. A.** 2008. The impact of inhaled corticosteroid and long-acting beta-agonist combination therapy on outcomes in COPD. Pulm. Pharmacol. Ther. **21:**540–550.
34. **Harcourt, J., R. Alvarez, L. P. Jones, C. Henderson, L. J. Anderson, and R. A. Tripp.** 2006. Respiratory syncytial virus G protein and G protein CX3C motif adversely affect CX3CR1$^+$ T-cell responses. J. Immunol. **176:**1600–1608.
35. **Harrod, K. S., R. J. Jaramillo, C. L. Rosenberger, S. Z. Wang, J. A. Berger, J. D. McDonald, and M. D. Reed.** 2003. Increased susceptibility to RSV infection by exposure to inhaled diesel engine emissions. Am. J. Respir. Cell Mol. Biol. **28:**451–463.
36. **Hayashida, S., K. S. Harrod, and J. A. Whitsett.** 2000. Regulation and function of CCSP during pulmonary *Pseudomonas aeruginosa* infection in vivo. Am. J. Physiol. Lung Cell. Mol. Physiol. **279:**L452–L459.
37. **Hegele, R. G., S. Hayashi, A. M. Bramley, and J. C. Hogg.** 1994. Persistence of respiratory syncytial virus genome and protein after acute bronchiolitis in guinea pigs. Chest **105:**1848–1854.
38. **Kahn, J. S.** 2006. Epidemiology of human metapneumovirus. Clin. Microbiol. Rev. **19:**546–557.
39. **Kolli, D., E. L. Bataki, L. Spetch, A. Guerrero-Plata, A. M. Jewell, P. A. Piedra, G. N. Milligan, R. P. Garofalo, and A. Casola.** 2008. T lymphocytes contribute to antiviral immunity and pathogenesis in experimental human metapneumovirus infection. J. Virol. **82:**8560–8569.
40. **Komatsu, T., K. Takeuchi, and B. Gotoh.** 2007. Bovine parainfluenza virus type 3 accessory proteins that suppress beta interferon production. Microbes Infect. **9:**954–962.
41. **Kraus, T. A., L. Garza, and C. M. Horvath.** 2008. Enabled interferon signaling evasion in an immune-competent transgenic mouse model of parainfluenza virus 5 infection. Virology **371:**196–205.
42. **Kuiken, T., B. G. van den Hoogen, D. A. van Riel, J. D. Laman, G. van Amerongen, L. Sprong, R. A. Fouchier, and A. D. Osterhaus.** 2004. Experimental human metapneumovirus infection of cynomolgus macaques (*Macaca fascicularis*) results in virus replication in ciliated epithelial cells and pneumocytes with associated lesions throughout the respiratory tract. Am. J. Pathol. **164:**1893–1900.
43. **Li, X. Q., Z. F. Fu, R. Alvarez, C. Henderson, and R. A. Tripp.** 2006. Respiratory syncytial virus (RSV) infects neuronal cells and processes that innervate the lung by a process involving RSV G protein. J. Virol. **80:**537–540.
44. **Lo, M. S., R. M. Brazas, and M. J. Holtzman.** 2005. Respiratory syncytial virus nonstructural proteins NS1 and NS2 mediate inhibition of Stat2 expression and alpha/beta interferon responsiveness. J. Virol. **79:**9315–9319.
45. **Mahalingam, S., J. Schwarze, A. Zaid, M. Nissen, T. Sloots, S. Tauro, J. Storer, R. Alvarez, and R. A. Tripp.** 2006. Perspective on the host response to human metapneumovirus infection: what can we learn from respiratory syncytial virus infections? Microbes Infect. **8:**285–293.
46. **Manoha, C., S. Espinosa, S. L. Aho, F. Huet, and P. Pothier.** 2007. Epidemiological and clinical features of hMPV, RSV and RVs infections in young children. J. Clin. Virol. **38:**221–226.
47. **Martin, J. G., S. Siddiqui, and M. Hassan.** 2006. Immune responses to viral infections: relevance for asthma. Paediatr. Respir. Rev. **7**(Suppl. 1)**:**S125–S127.
48. **Martinello, R. A., F. Esper, C. Weibel, D. Ferguson, M. L. Landry, and J. S. Kahn.** 2006. Human metapneumovirus and exacerbations of chronic obstructive pulmonary disease. J. Infect. **53:**248–254.
49. **Mazzoncini, J. P., Jr., C. B. Crowell, and C. S. Kang.** 2008. Human metapneumovirus: an emerging respiratory pathogen. J. Emerg. Med.
50. **McCullough, K. C.** 1983. Characterization of a non-syncytiogenic autonomously replicating variant of measles virus. J. Gen. Virol. **64**(Pt. 3)**:**749–754.
51. **McManus, T. E., A. M. Marley, N. Baxter, S. N. Christie, H. J. O'Neill, J. S. Elborn, P. V. Coyle, and J. C. Kidney.** 2008. Respiratory viral infection in exacerbations of COPD. Respir. Med. **102:**1575–1580.
52. **Mejias, A., S. Chavez-Bueno, A. M. Gomez, C. Somers, D. Estripeaut, J. P. Torres, H. S. Jafri, and O. Ramilo.** 2008. Respiratory syncytial virus persistence: evidence in the mouse model. Pediatr. Infect. Dis. J. **27:**S60–S62.
53. **Moore, E. C., J. Barber, and R. A. Tripp.** 2008. Respiratory syncytial virus (RSV) attachment and nonstructural proteins modify the type I interferon response associated with suppressor of cytokine signaling (SOCS) proteins and IFN-stimulated gene-15 (ISG15). Virol. J. **5:**116.
54. **Mullins, J. A., D. D. Erdman, G. A. Weinberg, K. Edwards, C. B. Hall, F. J. Walker, M. Iwane, and L. J. Anderson.** 2004. Human metapneumovirus infection among children hospitalized with acute respiratory illness. Emerg. Infect. Dis. **10:**700–705.
55. **Munir, S., C. Le Nouen, C. Luongo, U. J. Buchholz, P. L. Collins, and A. Bukreyev.** 2008. Nonstructural proteins 1 and 2 of respiratory syncytial virus suppress maturation of human dendritic cells. J. Virol. **82:**8780–8796.
56. **Parisien, J. P., J. F. Lau, and C. M. Horvath.** 2002. STAT2 acts as a host range determinant for species-specific paramyxovirus interferon antagonism and simian virus 5 replication. J. Virol. **76:**6435–6441.
57. **Rohde, G., I. Borg, U. Arinir, J. Kronsbein, R. Rausse, T. T. Bauer, A. Bufe, and G. Schultze-Werninghaus.** 2005. Relevance of human metapneumovirus in exacerbations of COPD. Respir. Res. **6:**150.
58. **Sabine Vollstedt, M. F., G. Alber, M. Ackermann, and M. Suter.** 2001. Interleukin-12- and gamma interferon-dependent innate immunity are essential and sufficient for long-term survival of passively immunized mice infected with herpes simplex virus type 1. J. Virol. **75:**9596–9600.
59. **Schowalter, R. M., S. E. Smith, and R. E. Dutch.** 2006. Characterization of human metapneumovirus F protein-promoted membrane fusion: critical roles for proteolytic processing and low pH. J. Virol. **80:**10931–10941.
60. **Schwarze, J., D. R. O'Donnell, A. Rohwedder, and P. J. Openshaw.** 2004. Latency and persistence of respiratory syncytial virus despite T-cell immunity. Am. J. Respir. Crit. Care Med. **169:**801–805.
61. **Sikkel, M. B., J. K. Quint, P. Mallia, J. A. Wedzicha, and S. L. Johnston.** 2008. Respiratory syncytial virus persistence in chronic obstructive pulmonary disease. Pediatr. Infect. Dis. J. **27:**S63–S70.
62. **Sin, D. D., and S. F. Man.** 2006. Corticosteroids and adrenoceptor agonists: the compliments for combination therapy in chronic airways diseases. Eur. J. Pharmacol. **533:**28–35.
63. **Skiadopoulos, M. H., S. Biacchesi, U. J. Buchholz, J. M. Riggs, S. R. Surman, E. Amaro-Carambot, J. M. McAuliffe, W. R. Elkins, M. St Claire, P. L. Collins, and B. R. Murphy.** 2004. The two major human metapneumovirus genetic lineages are highly related antigenically, and the fusion (F) protein is a major contributor to this antigenic relatedness. J. Virol. **78:**6927–6937.
64. **Spann, K. M., K. C. Tran, B. Chi, R. L. Rabin, and P. L. Collins.** 2004. Suppression of the induction of alpha, beta, and lambda interferons by the NS1 and NS2 proteins of human respiratory syncytial virus in human epithelial cells and macrophages. J. Virol. **78:**4363–4369.
65. **Tate, M. C., A. J. Garcia, B. G. Keselowsky, M. A. Schumm, D. R. Archer, and M. C. LaPlaca.** 2004. Specific beta1 integrins mediate adhesion, migration, and differentiation of neural progenitors derived from the embryonic striatum. Mol. Cell Neurosci. **27:**22–31.
66. **Tripp, R. A.** 2004. The brume surrounding respiratory syncytial virus persistence. Am. J. Respir. Crit. Care Med. **169:**778–779.
67. **Tripp, R. A., L. Jones, and L. J. Anderson.** 2000. Respiratory syncytial virus G and/or SH glycoproteins modify CC and CXC chemokine mRNA expression in the BALB/c mouse. J. Virol. **74:**6227–6229.
68. **Tripp, R. A., L. P. Jones, L. M. Haynes, H. Zheng, P. M. Murphy, and L. J. Anderson.** 2001. CX3C chemokine mimicry by respiratory syncytial virus G glycoprotein. Nat. Immunol. **2:**732–738.
69. **Tripp, R. A., D. Moore, L. Jones, W. Sullender, J. Winter, and L. J. Anderson.** 1999. Respiratory syncytial virus G and/or SH protein alters Th1 cytokines, natural killer cells, and neutrophils responding to pulmonary infection in BALB/c mice. J. Virol. **73:**7099–7107.
70. **Tripp, R. A., D. Moore, J. Winter, and L. J. Anderson.** 2000. Respiratory syncytial virus infection and G and/or SH protein expression contribute to substance P, which mediates inflammation and enhanced pulmonary disease in BALB/c mice. J. Virol. **74:**1614–1622.
71. **Tripp, R. A., C. Oshansky, and R. Alvarez.** 2005. Cytokines and respiratory syncytial virus infection. Proc. Am. Thorac. Soc. **2:**147–149.
72. **Valdovinos, M. R., and B. Gomez.** 2003. Establishment of respiratory syncytial virus persistence in cell lines: association with defective interfering particles. Intervirology **46:**190–198.
73. **van den Hoogen, B. G., J. C. de Jong, J. Groen, T. Kuiken, R. de Groot, R. A. Fouchier, and A. D. Osterhaus.** 2001. A newly discovered human pneumovirus isolated from young children with respiratory tract disease. Nat. Med. **7:**719–724.
74. **van den Hoogen, B. G., S. Herfst, M. de Graaf, L. Sprong, R. van Lavieren, G. van Amerongen, S. Yuksel, R. A. Fouchier, A. D. Osterhaus, and R. L. de Swart.** 2007. Experimental infection of macaques with human metapneumovirus induces transient protective immunity. J. Gen. Virol. **88:**1251–1259.

75. **van den Hoogen, B. G., D. M. Osterhaus, and R. A. Fouchier.** 2004. Clinical impact and diagnosis of human metapneumovirus infection. Pediatr. Infect. Dis. J. **23:**S25–S32.
76. **Varkey, J. B., and B. Varkey.** 2008. Viral infections in patients with chronic obstructive pulmonary disease. Curr. Opin. Pulm. Med. **14:**89–94.
77. **Wilkinson, K. D., K. M. Lee, S. Deshpande, P. Duerksen-Hughes, J. M. Boss, and J. Pohl.** 1989. The neuron-specific protein PGP 9.5 is a ubiquitin carboxyl-terminal hydrolase. Science **246:**670–673.
78. **Wilkinson, T. M., G. C. Donaldson, S. L. Johnston, P. J. Openshaw, and J. A. Wedzicha.** 2006. Respiratory syncytial virus, airway inflammation, and FEV1 decline in patients with chronic obstructive pulmonary disease. Am. J. Respir. Crit. Care Med. **173:**871–876.
79. **Wolf, D. G., D. Greenberg, D. Kalkstein, Y. Shemer-Avni, N. Givon-Lavi, N. Saleh, M. D. Goldberg, and R. Dagan.** 2006. Comparison of human metapneumovirus, respiratory syncytial virus and influenza A virus lower respiratory tract infections in hospitalized young children. Pediatr. Infect. Dis. J. **25:**320–324.
80. **Zheng, H., G. A. Storch, C. Zang, T. C. Peret, C. S. Park, and L. J. Anderson.** 1999. Genetic variability in envelope-associated protein genes of closely related group A strains of respiratory syncytial virus. Virus Res. **59:**89–99.